Dehydrozaluzanin C- derivative protects septic mice by alleviating over-activated inflammatory response and promotes the phagocytosis of macrophages

Ying-xiang Zou[1,2,#], Tian-nan Xiang[5,1,2,#], Li-rong Xu[1,2], Huan Zhang[1,2], Yu-he Ma[1,2], Lu Zhang[1,2], Chun-xian Zhou[1,2], Xiao Wu[1,2], Qi-lin Huang[1,2], Biao Lei[1,2], Jing-wen Mu[1,2], Xiang-yang Qin[4,*], Xin Jiang[1,2,*], Yue-juan Zheng[1,2,3,*]

[1]School of Integrative Medicine, Shanghai University of Traditional Chinese Medicine, Shanghai 201203, China

[2]The Research Center for Traditional Chinese Medicine, Shanghai Institute of Infectious Diseases and Biosecurity, Shanghai University of Traditional Chinese Medicine, Shanghai, 201203, China

[3]Shanghai Key Laboratory of Health Identification and Assessment, Shanghai University of Traditional Chinese Medicine, Shanghai 201203, China

[4]Department of Chemistry, school of pharmacy, Furth Military University, Xi'an, Shaanxi, 710032, China

[5]Department of Chinese Medicine, Hubei College of Chinese Medicine, Jingzhou, Hubei, 434020, China

[#]These authors contributed equally to this work.

[*] **Correspondence**: Prof. Yue-juan Zheng and Prof. Xin Jiang, School of Integrative Medicine, Shanghai University of Traditional Chinese Medicine, Shanghai, 201203, China. Tel: (+86)21-5132 2134, Fax: (+86)-21-5132 2130, Email: 13641776412@163.com (Yue-juan Zheng), and jiangxingao@163.com (Xin Jiang).

Prof. Xiang-yang Qin, Department of Chemistry, school of pharmacy, Furth Military University, Xi'an, Shaanxi 710032, China. Tel: (+86) 029-8477 4473, Fax: (+86) 029-8477 4473, Email: qinxiangyang@fmmu.edu.cn.

Abstract

In the course of sepsis, excessive inflammatory response can lead to cytokine storm. The severity of cytokine storm is closely related with poor prognosis. Dehydrozaluzanin C-derivative (DHZD) is a modified compound from *Magnolia officinalis*. Here, we demonstrated that DHZD ameliorated tissue damage (lung, kidney and liver) and excessive inflammatory response induced by LPS challenge or the infection of *Carbapenem-resistant Klebsiella pneumoniae* (CRKP). In LPS-induced sepsis model, DHZD could reduce the secretion of inflammatory factors IL-6, TNF-α, etc. and increased the survival rate. *In vitro* experiments, DHZD also decreased LPS-stimulated expression of IL-6, TNF-α and MCP-1 via PI3K/Akt/p70S6K signaling pathway in macrophages, etc., might accounting for the decreased tissue damage and its protective role *in vivo*. Interestingly, the combined treatment group of DXM and DHZD had higher survival rate and lower level of IL-6 than those of DXM-treated group. The combination of DHZD and DXM played a synergistically role to decrease IL-6 secretion in sera. DHZD not only improved the hypothermic symptoms of acute peritonitis induced by CRKP, but also inhibited heat-killed CRKP-induced inflammatory response in macrophages. Similar to that of DXM-treated group, the proportions of phagocytic cell types, e.g., neutrophils and monocytes/macrophages in lungs were upregulated by DHZD. What's more, the phagocytic receptor CD36 was

increased by DHZD in macrophages, which was accompanied by increased bacterial phagocytosis in clathrin- and actin-dependent manner. In short, DHZD is a potential drug candidate with host-directed immunomodulatory effects during bacterial infection through increasing the numbers and the phagocytic ability of phagocytes and decreasing their inflammatory responses together.

Key words: DHZD, sepsis, CRKP, phagocytosis, cytokine storm

Introduction

Sepsis is a life-threatening syndrome of multiple organ dysfunction, which is usually caused by bacterial infection, etc. Gram-negative (G^-) bacteria account for a large proportion of severe sepsis, which is a serious threat to global public health and economic burden (1, 2). The incidence of sepsis is much higher than myocardial infarction (3) or the combination of prostate, breast, and lung cancer (4). As reported, there are 15 to 30 million cases of sepsis worldwide every year (5, 6). The mortality rate is close to 20 %. In recent decades, antimicrobial resistance (AMR) poses an increasing threat to global public health. CRKP is an important strain in clinical practice, which can cause severe nosocomial infections, such as sepsis, pneumonia, urinary tract infection, surgical site infection and soft tissue infection [11]. CRKP accounts for about 64 % of carbapenem-resistant enterobacterial infections in China [12].

The current clinical treatment for sepsis caused by bacterial infection mainly relies on antibiotic therapy to control the infection and the use of glucocorticoid to inhibit excessive inflammatory response. Glucocorticoids (such as dexamethasone) are effective in treating sepsis, but they also accelerate the apoptosis of specific immune

67 cells. Side effects of long-term glucocorticoid use include osteoporosis (7) or
68 opportunistic infections due to its immunosuppressive effects (8). However, the
69 development of new antimicrobial drugs, especially targeting G^- bacteria, lags behind
70 the emergence of antibiotic resistance obviously, which has become a major obstacle in
71 the clinic. New drug candidates are eagerly wanted.

72 As a major component of the cell wall of G^- bacteria, lipopolysaccharide (LPS) is
73 one of the most important pathogen-associated molecular patterns, and can elicit
74 inflammatory immune response via Toll-like receptor 4 (TLR4) in various immune cells
75 (9). After ligation of TLR4, adaptor molecules such as myeloid differentiation protein
76 88 (MyD88), interleukin-1 (IL-1) receptor-associated kinases (IRAKs), tumor necrosis
77 factor (TNF) receptor-associated factor 6 (TRAF6), transforming growth factor (TGF)-
78 activated kinase 1 (TAK1), and subsequent MAPKs and nuclear factor κB (NF-κB) are
79 activated. Excessive inflammation can lead to "cytokine storm", commonly known as
80 systemic inflammatory response syndrome (SIRS). The pathologic progress of sepsis
81 is usually accompanied by SIRS. The uncontrolled inflammatory response usually
82 causes organ dysfunction, multiple organ failure and even death (10).

83 Besides the inflammatory immune damage, the poor clearance of pathogens is
84 usually associated with poor prognosis during bacterial infection.
85 Monocytes/macrophages, and dendritic cells (DCs) are the main phagocytes to
86 phagocytize bacteria and present their antigens to T cells (11). Neutrophil is also an
87 important cell type of phagocytes. The progress of phagocytosis includes 3 stages:
88 receptor-mediated, membrane fusion, and actin-driven (12). There are a variety of

89 phagocytic receptors, including C-type lectin receptors (CLRs), mannose receptors,
90 scavenger receptors (SR-A1, MARCO and CD36), complement receptors (CR3 and
91 CR4) and Fc receptors (12-14).

92 Host-directed therapy (HDT) is a new adjuvant therapy strategy especially for the
93 treatment of severe infection. It is not mediated by killing pathogens directly, but
94 promoting the immune clearing of pathogens through phagocytes, and/or reduces tissue
95 damage caused by excessive inflammatory response. Thus, HDT drug candidates could
96 play a protective role for the treatment of bacterial infection from the aspect of host.

97 In our previous work, dehydrozaluzanin C (DHZC), a sesquiterpenoid from
98 *Magnolia officinalis*, has strong anti-inflammatory activity but its drug toxicity is
99 relatively high. DZHD is a modified compound from DHZC by decreasing cytotoxicity
100 and increase the druggability.

101 In this study, the protective effects of DHZD on mice in lethal LPS challenge or
102 CRKP-infected septic mouse models and the underlying mechanisms were
103 demonstrated.

104 **Materials and methods**

105 **Animals and reagents**

106 Six-week-old wild-type female C57BL/6J mice (18 ± 2 g) were obtained from
107 Joint Ventures Sipper BK Experimental Animal Co. (Shanghai, China). All mice had
108 free access to food and water during all the experiments and were housed in a 12/12 h
109 light/dark cycle. The experimental procedures were approved by the Experimental
110 Animal Ethical Committee, Shanghai University of Traditional Chinese Medicine

111 (Shanghai, China) (PZSHUTCM220307018).

112 DHZD was modified from DHZC isolated from *Magnolia officinalis*. LPS (0111:
113 B4), DMSO, dexamethasone (DXM) and chlorpromazine hydrochloride (CPZ) were
114 purchased from Sigma (St. Louis, MO, USA). Cell counting kit 8 (CCK-8) were
115 obtained from Meilunbio (Dalian, China). Enzyme-linked immunosorbent assay
116 (ELISA) kits for mouse IL-6, TNF-α, MCP-1, IL-10 IFN-β, and granulocyte-
117 macrophage colony stimulating factor (mGM-CSF) were purchased from R&D
118 Systems (Minneapolis, MN, USA). Mouse recombinant cytokine IL-4 were from
119 Peprotech (USA). The detection kit of nitric oxide (NO) was obtained from Beyotime
120 Biotechnology (Shanghai, China). FITC anti-mouse CD11c, APC anti-mouse CD40,
121 APC/Fire™ 750 anti-mouse CD80, PerCP/Cyanine5.5 anti-mouse CD86, Brilliant
122 Violet 421™ anti-mouse I-A/I-E, FITC anti-mouse CD45, Brilliant Violet 650 Ly6G,
123 Brilliant Violet 421 Ly6C and PE/Cyanine7 F4/80 were purchased from Biolegend
124 (USA). Dexamethasone sodium phosphate injection was from Sinopharm (China).
125 SYBR RT-PCR Kit was purchased from Takara (Dalian, China). PHrodo-labelled
126 *E. coli* was purchased from ThermoFisher (USA). Cytochalasin D was obtained from
127 Abcam (USA). Filipin III was from MCE (USA). Levofloxacin (LVX) and meropenem
128 (MEM) were obtained from the National Institute for Food and Drug Control of China
129 (Beijing, China) CRKP (HS11286) was kindly provided by Dr. Yi-jian Chen from
130 Huashan Hospital affiliated to Fudan University.

131 **Cell culture**

132 Mouse macrophage-like cell line RAW264.7 were purchased from ATCC

133 (Manassas, VA, USA) and cultured as previously described (15).

134 Thioglycolate-elicited mouse primary peritoneal macrophages were isolated from
135 female C57BL/6J mice at 6-8 weeks of age and cultured in DMEM (GE, USA) with
136 10 % FBS (Biowest, France) and 1 % Penicillin-Streptomycin, as previously described
137 (16).

138 Bone marrow-derived macrophages (BMDMs) and bone marrow-derived
139 dendritic cells (BMDCs) were both obtained from C57BL/6J mice (4 weeks old). The
140 BMDMs were cultured in DMEM containing 10 ng/mL M-CSF (Peprotech, USA) and
141 10 % FBS. The BMDCs were differentiated in RPMI 1640 (GE, USA) medium
142 containing 10 % FBS, 50 ng/mL mGM-CSF (R&D Systems, USA) and 4 ng/mL mIL-
143 4 (Peprotech, USA).

144 **Cell viability assay**

145 RAW264.7 cells (1×10^5 cells/well) were cultured in 96-well plates overnight and
146 treated with different concentrations of DHZD (0-15 μM) in 12, 24, 48 and 72 h. The
147 cytotoxicity of DHZD was evaluated by CCK-8 counting kit according to the
148 manufacturer's instructions (Meilunbio, Dalian, China).

149 **Enzyme-linked immunosorbent assay**

150 The inflammatory factors (IL-6, TNF-α, MCP-1, IL-10 and IFN-β) in the cell
151 culture supernatants were detected by ELISA (R&D Systems, USA).

152 Blood samples were collected at 12 h after LPS challenge and allowed to clot for
153 3 h followed by centrifugation at 3500 rpm for 25 min (4 °C) to prepare serum sample.
154 Serum inflammatory cytokines (IL-6, TNF-α, MCP-1 and IL-10) were measured by

155 corresponding ELISA kit (R&D Systems, USA) according to the manufacturer's
156 instructions.

157 **Assessment of nitric oxide (NO) level**

158 Quantitative detection of NO was carried out by NO detection kit (S0021) which
159 was purchased from Beyotime Biotechnology (Shanghai, China).

160 **Detection of MHC II and co-stimulatory molecules on BMDCs**

161 Bone marrow stem cells were derived and differentiated into BMDCs. After 5 days,
162 BMDCs were seeded in 12-well plates overnight. LPS (100 ng/mL) and DHZD (15 μM)
163 were added into culture medium of BMDCs for another 24 h. Then BMDCs were
164 harvested and labeled with FITC anti-mouse CD11c (Biolegend, 117305, USA), APC
165 anti-mouse CD40 (Biolegend, 124611, USA), APC/Fire™ 750 anti-mouse CD80
166 (Biolegend, 104739, USA), PerCP/Cyanine5.5 anti-mouse CD86 (Biolegend, 105027,
167 USA) and Brilliant Violet 421™ anti-mouse I-A/I-E (Biolegend, 107631, USA). And
168 then cells were analyzed by Flow cytometry (Beckman, USA), and data were analyzed
169 using FlowJo software.

170 **The establishment of septic mice by lethal dose of LPS challenge**

171 The septic mouse model was established by intraperitoneal injection of LPS (12.5
172 mg/kg, Sigma) as described (17, 18). Six groups were included: LPS group, LPS +
173 DXM group (5 mg/kg), LPS + DHZD group (10 mg/kg), LPS + DHZD group (20
174 mg/kg), LPS + DHZD group (40 mg/kg) and LPS + MEM (5 mg/kg) + DHZD group
175 (10 mg/kg). The survival statuses of mice in different groups were recorded at different
176 intervals as described previously (19).

RNA extraction and real-time PCR

Total RNA was extracted from lung tissues or different types of cells and reverse-transcribed into cDNA. Real-time PCR was performed with SYBR RT-PCR kit (Takara, Dalian, China). The mRNA levels were normalized against β-Actin and presented as $2^{-\Delta\Delta Ct}$. The primer sequences for qRT-PCR amplification were as the following:

mβ-Actin	mβ-Actin-F	5’-AGTGTGACGTTGACATCCGT-3’
	mβ-Actin-R	5’-GCAGCTCAGTAACAGTCCGC-3’
mIL-6	mIL-6F	5’-TAGTCCTTCCTACCCCAATTTCC-3’
	mIL-6R	5’-TTGGTCCTTAGCCACTCCTTC-3’
mTNF-α	mTNF-αF	5’-AAGCCTGTAGCCCACGTCGTA-3’
	mTNF-αR	5’-GGCACCACTAGTTGGTTGTCTTTG-3’
mMCP-1	mMCP-1F	5’- GCATCCACGTGTTGGCTCA -3’
	mMCP-1R	5’- CTCCAGCCTACTCATTGGGATCA -3’
mMIP-2	mMIP-2-F	5’-CACTCTCAAGGGCGGTCAA-3’
	mMIP-2-R	5’-AGGCACATCAGGTACGATCCA-3’
mIL-10	mIL-10F	5’-GCTCTTACTGACTGGCATGAG-3’
	mIL-10R	5’-CGCAGCTCTAGGAGCATGTG-3’
mCD206	mCD206F	5’-CTCTGTTCAGCTATTGGACGC-3’
	mCD206R	5’-TGGCACTCCCAAACATAATTTGA-3’
mDectin-1	mDectin-1F	5’-AGGCATCCCAAACTACAGGAG-3’
	mDectin-1R	5’-GGAGCAGTGTCTCTTACTTCCAT-3’
mCR3	mCR3F	5’- CCATGACCTTCCAAGAGAATGC -3’

	mCR3R	5’- ACCGGCTTGTGCTGTAGTC -3’
mCR4	mCR4F	5’- CTGGATAGCCTTTCTTCTGCTG -3’
	mCR4R	5’- GCACACTGTGTCCGAACTCA -3’
mFcγR2a	mFcγR2aF	5’-TGGACAGCCGTGCTAAATCTT-3’
	mFcγR2aR	5’-GGTCCCTTCGCATGTCAGTG-3’

Flow cytometry

The left lungs of mice in the different groups were collected at 12 h after LPS challenge, and the lung tissues were snipped and digested with collagenase (Sigma Aldrich) and DNase I (Sigma Aldrich) in gentleMACS^{TM} (Miltenyi, Germany) at 80 rpm (37 °C) for 55 min. After digestion, the samples were filtered through a 40 mm filter using a syringe piston, and centrifuged at 1000 rpm (4 °C) for 5 min. RBC lysis buffer (BD Biosciences, USA) was added to cell pellets at room temperature for 5 min, and then PBS (8 mL) was added and centrifuged at 1400 rpm (4 °C) for 5 min. Cells were counted and then incubated at 4 °C for 25 min with FITC anti-mouse CD45 (Biolegend, 103107, USA), Brilliant Violet 650 Ly6G (Biolegend, 127641, USA), Brilliant Violet 421 Ly6C (Biolegend, 128031, USA) and PE/Cyanine7 F4/80 (Biolegend, 123113, USA) antibodies. Samples were run on CytoFlex LX (Beckman, USA). Data were analyzed using FlowJo software.

Detection of the phagocytosis of macrophages

The phagocytosis of pHrodo labelled *E. coli* (ThermoFisher, California, USA) was detected in RAW264.7 cells by Flow cytometry. Cells were stimulated by DHZD (15 μM) with or without LPS (100 ng/mL) for 24 h, and then co-incubated with pHrodo-

199 labelled *E. coli* (10 μL/well) at 37 °C for 1 h. RAW264.7 cells were pretreated by 3 μM
200 of Filipin III (MCE, USA), 10 μM of chlorpromazine hydrochloride (Sigma, USA) or
201 10 μM of cytochalasin D (Abcam, USA) for 30 min, and then pHrodo labelled *E. coli*
202 were added for another 1 h. The phagocytosis of *E. coli* was investigated by BD
203 Accuri^{TM} C6 Flow cytometry (BD, USA), and data were analyzed by FlowJo software.

204 **Western blot**

205 The phosphorylation of important signaling proteins from RAW264.7 cells and
206 their corresponding total proteins were determined by Western blot as previously
207 described (20). All the antibodies were bought from Cell Signaling Technology
208 (Beverly, MA, USA).

209 **CRKP-induced septic mouse model**

210 The septic mouse model was established by intraperitoneal injection of CRKP
211 (9×10^7 CFU/mouse) in 0.4 mL of PBS. The experiments were carried out in the
212 following groups: CRKP group, CRKP + MEM (5 mg/kg) group, CRKP + LVX (75
213 mg/kg) group, CRKP + DHZD group (20 mg/kg), CRKP + DHZD group (40 mg/kg)
214 and the combined treatment CRKP + DHZD (20 mg/kg) + MEM (5 mg/kg) group. The
215 body temperature of mice was recorded by infrared body thermometer (HJKIR, Wuhan)
216 before or 9 hours after injection of CRKP.

217 **Preparation of HK-CRKP**

218 Monoclonal colonies were picked from the CRKP bacterial culture plates and
219 cultured in LB medium for 12 h at 37°C on a constant temperature shaker. After heating
220 1 mL of the bacterial solution in a 65°C water bath for 45 min, the solution was

221 centrifuged (4400 rpm×15 min), resuspended in sterile PBS, centrifuged again (4400
222 rpm×15 min), and resuspended in DMEM for further use (MOI=10).

223 **Histopathology**

224 Hematoxylin and eosin (H&E) were used to measure the pathological damage of
225 lungs, livers and kidneys. After 12 h of LPS challenge (10 mg/kg), mice were sacrificed
226 and lung, liver and kidney tissues were collected to be fixed with 4 % formaldehyde
227 and paraffin-embedded.

228 CRKP-induced (6×10^7 CFU/mouse) peritonitis mouse model was carried out with
229 C57BL/6J mice and different groups were treated as indicated. After 12 h, mice were
230 sacrificed and lungs and livers were collected to be fixed with 4 % formaldehyde and
231 embedded in paraffin.

232 All of the above tissues were sliced and stained with H&E. The histopathological
233 changes were observed using a PANNORAMIC MIDI II microscope (3DHistech,
234 Hungary). Pulmonary edema, alveolar infiltration, and pulmonary vasculitis were
235 scored on a 12-point pathological scale (21).

236 **Statistical analysis**

237 Statistical analysis was performed using GraphPad Prism 9. Data were presented
238 as means ± standard deviation (SD). Student's *t*-test analyses was used to evaluate the
239 comparisons between two groups. Comparisons multiple groups were evaluated by
240 one-way ANOVA followed by Tukey's post hoc comparisons, respectively. *P* values
241 were considered as *, $P<0.05$; **, $P<0.01$; ***, $P<0.001$; ****, $P<0.0001$.

242 **Results**

243 **DHZD inhibited the secretion of LPS-induced cytokines in RAW264.7 cells**

244 CCK-8 kit was used to determine whether DHZD affected cell viability. The
245 structure of DHZD was shown in Fig. 1A. DHZD was synthesized according to the
246 previously reported method (22). Spectroscopic data were in accordance with reported
247 values (Supplementary Fig.1)(22). DHZD (0-15 μM) did not affect the proliferation of
248 RAW264.7 cells within 72 h. At the same time, DHZD inhibited LPS-induced secretion
249 of IL-6, TNF-α, MCP-1, IFN-β, and IL-10 in a dose-dependent manner (Fig. 1B-H).

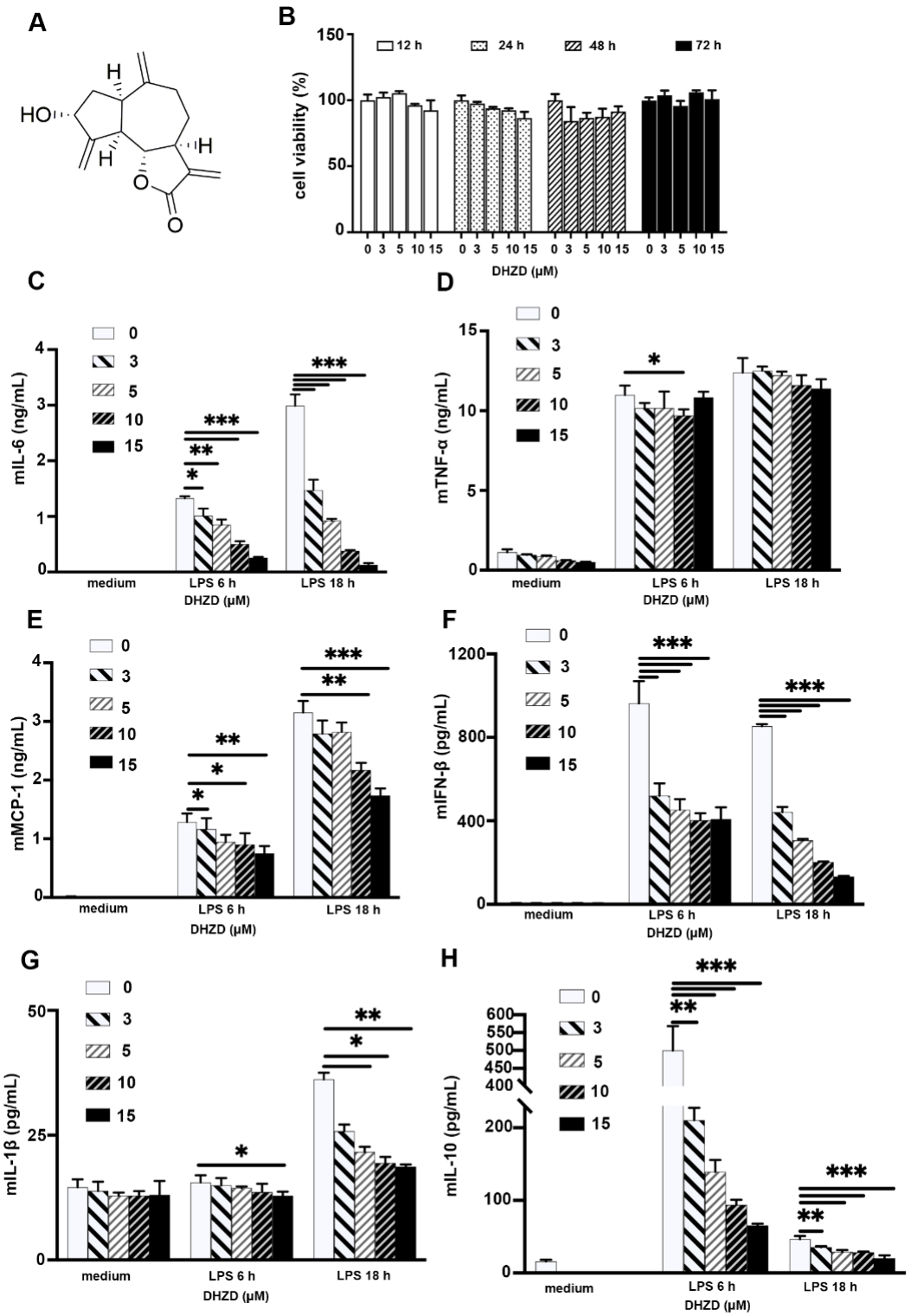

Figure 1. DHZD inhibited the secretion of LPS-induced cytokines in RAW264.7 cells. RAW264.7 were co-cultured with different concentrations of DHZD, and the absorbance at 450 nm at 12, 24, 48, 72 h to calculate the cell survival rate according to the formula (B). RAW264.7 (2×10^5 cells/well) were plated as indicated and administrated with DHZD and/or LPS (100 ng/mL) for 6 h

255 and 18 h. ELISA was carried out to detect the secretion of IL-6 (C), TNF-α (D), MCP-1 (E), IFN-β
256 (F), IL-1β (G) and IL-10 (H) in the cell culture supernatants. Values are means of three replicate
257 determinations (n=3) ± SD. *, $P<0.05$, **, $P<0.01$, and ***, $P<0.001$.

258 **DHZD suppressed the secretion of LPS-induced expression of IL-6, TNF-α, MCP-**
259 **1, IL-1β, IFN-β and IL-10 in mouse primary macrophages**

260 Compared to macrophage-like cell line, the biological activities of primary
261 macrophages are closer to the physiological and pathological characteristics of
262 macrophages *in vivo*. Therefore, mouse primary peritoneal macrophages and BMDMs
263 were used to validate the anti-inflammatory effects of DHZD. DHZD was also able to
264 inhibit the secretion of LPS-induced pro-inflammatory mediators IL-6, TNF-α, IL-1β,
265 IFN-β, NO, MCP-1 and anti-inflammatory cytokine IL-10 (Fig. 2A-G). Similarly,
266 DHZD decreased the secretion of IL-6, TNF-α and IL-10 after LPS stimulation in
267 BMDMs (Supplementary Fig. 2A-C).

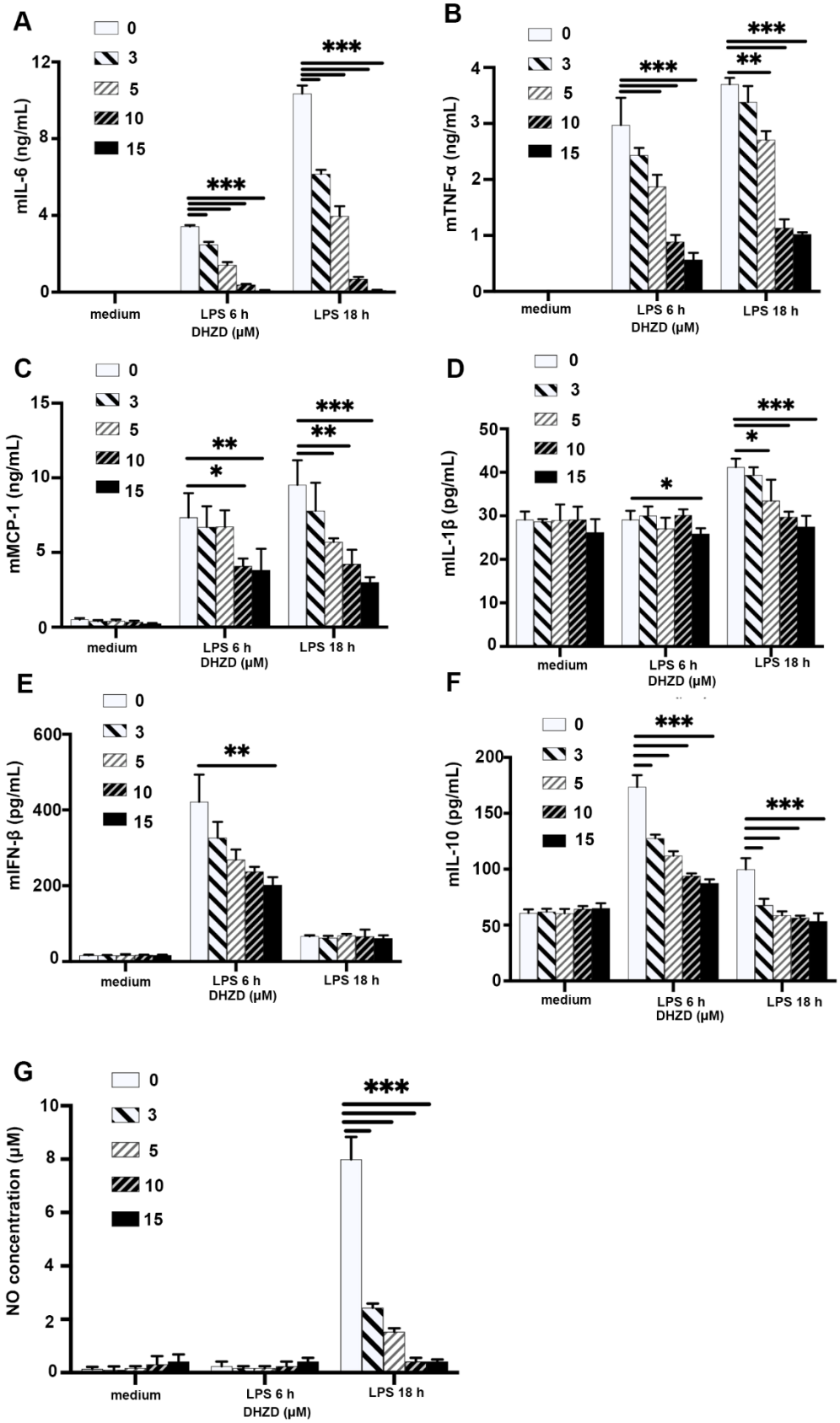

268

269 **Figure 2. DHZD suppressed the secretion of LPS- induced expression of IL-6, TNF-α, MCP-**

1, IL-1β, IFN-β and IL-10 in mouse primary macrophages. Mouse primary macrophages were plated (3.5×10^5 cells/500 μL) in 24-well plates at the day before stimulated. Cell culture supernatants were collected at 6 h and 18 h after co-stimulation of different concentrations of DHZD and LPS (100 ng/mL), and the concentrations of IL-6 (A), TNF-α (B), MCP-1 (C), IL-1β (D), IFN-β (E), IL-10 (F) and NO (G) were measured by ELISA. Data are means of three replicate determinations ± SD (n=3). *, P <0.05, **, P <0.01, and ***, P <0.001.

DHZD decreased LPS-induced secretion of inflammatory cytokines in BMDCs, and DHZD also downregulated the expression of MHC II and co-stimulatory molecules on the surface of BMDCs

DCs are the most important and powerful antigen presenting cells to activate naive T cells, bridging innate immunity and adaptive immunity. They participate in the phagocytosis, digestion of bacteria and presenting their antigens to evoke T cell immunity. During the transition of DCs from immature to mature status, co-stimulatory molecules are upregulated, downregulating the phagocytosis and promoting the antigen presenting ability, demonstrating the biological function of DCs. Meanwhile, DCs also secret inflammatory cytokines (IL-6, TNF-α, IL-12 and a variety of chemokines), contributing to the formation of cytokine storm together with activated T cells during the pathological progress of sepsis. DHZD reduced the secretion of IL-6, TNF-α, and IL-12p70 (Fig. 3A-C) induced by LPS.

In order to investigate whether DHZD has a regulatory effect on the antigen presentation function of DCs, thereby affecting the activation of T cells, Flow cytometry was used to detect LPS-stimulated expression of costimulatory molecules

292 (CD80, CD86, and CD40) and MHC Class II molecule (Iab). DHZD inhibited the

293 expression of these molecules (Fig. 3D-G).

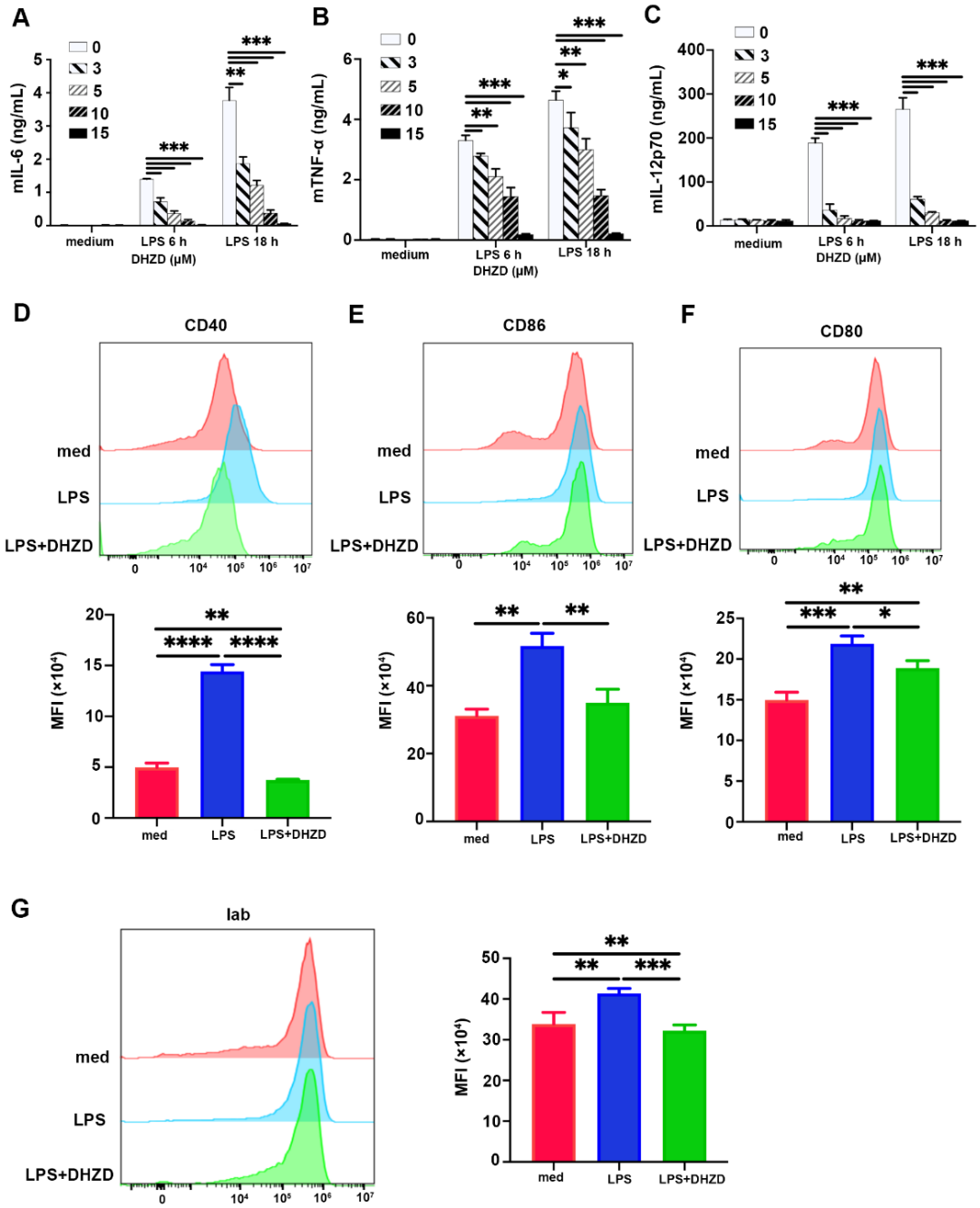

294

295 **Figure 3. DHZD decreased LPS-induced secretion of inflammatory cytokines in BMDCs, and**

296 **DHZD also downregulated the expression of MHC II and co-stimulatory molecules on the**

297 **surface of BMDCs.** Mouse bone marrow-derived dendritic cells were seeded at 3.5 × 10^5 cells/500

298 μL in 24-well plates along with stimulation by DHZD (0-15 μM) with or without LPS (100 ng/mL)
299 for 6 h or 18 h. The production of IL-6 (A), TNF-α (B) and IL-12p70 (C) in cell culture supernatants
300 were detected by ELISA. BMDCs were seeded in 12-well plate and treated with or without LPS
301 (100 ng/mL) along with DHZD (15 μM) for another 24 h. The expression of costimulatory
302 molecules CD40 (D), CD86 (E), CD80 (F) and antigen-presenting molecule MHC II (Iab) (G) was
303 quantified by FACS and the MFI (mean fluorescence intensity) of each sample was analyzed using
304 FlowJo. Data were show as mean ± SD of three separated experiments. *, $P<0.05$, **, $P<0.01$, ***,
305 $P<0.001$, and ****, $P<0.0001$.

306 **DHZD protected septic mice by inhibiting the over-activated inflammatory**
307 **response**

308 To determine the protective role of DHZD against LPS-induced (12.5 mg/kg)
309 septic shock, a survival analysis was carried out. DXM, a glucocorticoid used in the
310 clinical treatment of bacterial infection, was used as a positive control drug.

311 All mice in the model group died within 40 h. 60 % of mice in DXM treatment
312 group survived, 10 % of mice in low dose DHZD treatment group survived, 30 % of
313 mice in medium or high dose DHZD treatment group survived at the end of observation.
314 However, 100 % of mice in low dose DHZD and DXM treatment group survived (Fig.
315 4A).

316 In the control group, the lung, liver and kidney tissue structure were intact. On the
317 contrary, after LPS challenged, the lung tissue pathology of mice showed obvious
318 infiltration of inflammatory cells, a large amount of fluid exudation in the alveoli, and
319 lung interstitial thickening. The liver tissue also showed obvious inflammatory cell

320 infiltration, swelling and necrosis of hepatocytes, fragmentation and dissolution of
321 some nuclei, and destruction of the hepatic plate structure. The renal tissue also showed
322 obvious inflammatory cell infiltration, degeneration and necrosis of renal tubular
323 epithelial cells, and narrowing of renal cysts. The destruction of lung, liver and kidney
324 tissue structure was improved after DHZD treatment (Fig. 4B). DHZD was found to
325 improve pulmonary edema, alveolar infiltration, and pulmonary vasculitis by
326 pathological score of lung tissue (Fig. 4C).

327 Multiple organ failure caused by a "cytokine storm" during infection is the leading
328 cause of death in sepsis patients. In septic mice model of LPS-induced (10 mg/kg),
329 DHZD and DXM suppressed LPS-induced production of IL-6, TNF-α, MCP-1 and IL-
330 10. Compared with DXM treatment group, the combination treatment could
331 significantly inhibit the secretion of these cytokines (Fig. 4D-G).

332 Sepsis induced by bacterial infection can cause systemic organ dysfunction, and
333 lungs are often the most easily affected important organs. Therefore, Sepsis is often
334 accompanied by acute lung injury (ALI) or acute respiratory distress syndrome (ARDS),
335 which is one of the most important prognostic factors of sepsis death. We detected the
336 expression of lung inflammatory factors by qPCR, and found that both DHZD
337 administration group and combined administration group could significantly inhibit the
338 production of proinflammatory cytokines IL-6, chemokines MCP-1 and MIP-2 in the
339 lungs of mice (Supplementary Fig. 3A-C).

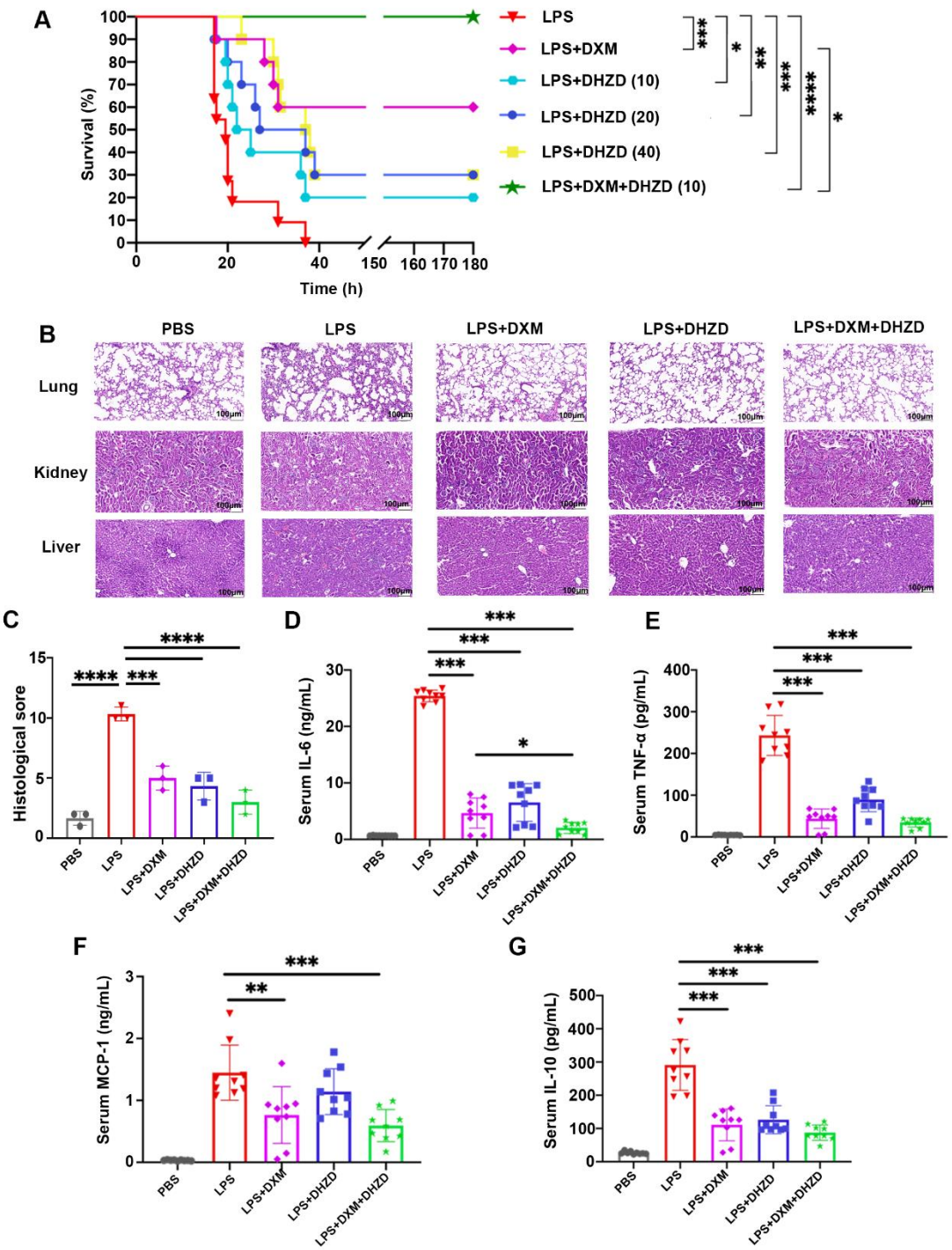

Figure 4. DHZD protected septic mice by inhibiting the over-activated inflammatory response. C57BL/6J female mice were randomly divided into 6 groups (10 mice/group). All groups of mice were challenged by lethal dose of LPS (12.5 mg/kg, ip) and corresponding agents, respectively. Survival status of different groups were recorded every 2-3 h in the following continuous 180 h (A). Data were analyzed using Log-Rank test and survival curve was generated by GraphPad Prism 9.0.

346 C57BL/6J mice were randomly divided into 5 groups (9 mice/group). All groups of mice were
347 infected with LPS (10 mg/kg, ip) group，PBS group, LPS + DXM (5 mg/kg) group, LPS + DHZD
348 (40 mg/kg) group and LPS + DXM (5 mg/kg) + DHZD (10 mg/kg) group. After 12 h of intervention,
349 blood samples were collected from eyeball. H&E staining of lung, kidney and liver (100×) (B).
350 Scale bar 100 μm, and the histological core of lung (C). The serum levels of IL-6 (D), TNF-α (E),
351 MCP-1 (F) and IL-10 (G) were measured by ELISA. Data were shown as mean ± SD of nine mice
352 per group. *, P <0.05, **, P <0.01, ***, P <0.001, and ****, P <0.0001.

353 **DHZD increased the cell numbers of lung neutrophils, monocytes and**
354 **macrophages induced by LPS challenge**

355 In most cases, locally recruited natural immune cells (such as neutrophils and
356 monocytes/macrophages) can rapidly phagocyte bacteria, control the bacterial load in
357 tissues, and reduce the occurrence of severe infection. However, when severe infection
358 occurs, a large number of immune cells participate in the secretion of inflammatory
359 cytokines, forming cytokine storms, which can lead to organ damage, sepsis and even
360 death. Thus, in the early stage of infection, rapid phagocytosis and elimination of
361 bacteria, and subsequently control of the body's immune response within reasonable
362 limitation, are the key aspects for treatment.

363 The infiltration of neutrophils and monocytes/macrophages in the lungs were
364 measured by Flow cytometry. As shown in Figure 5, at 12 h after LPS injection, the
365 ratio of neutrophils (Fig. 5A-C), monocytes/macrophages (Fig. 5D-H) increased in
366 DHZD-treated group and in DHZD + DXM group compared to LPS challenged group,
367 suggesting an increase in the number of innate immune cells with the ability to

368 phagocyte bacteria. It may be beneficial to play a rapid phagocytic role in the early

369 stage of bacterial infection, reducing the bacterial load and the severity of infection in

370 tissues, and thus play a potential protective role.

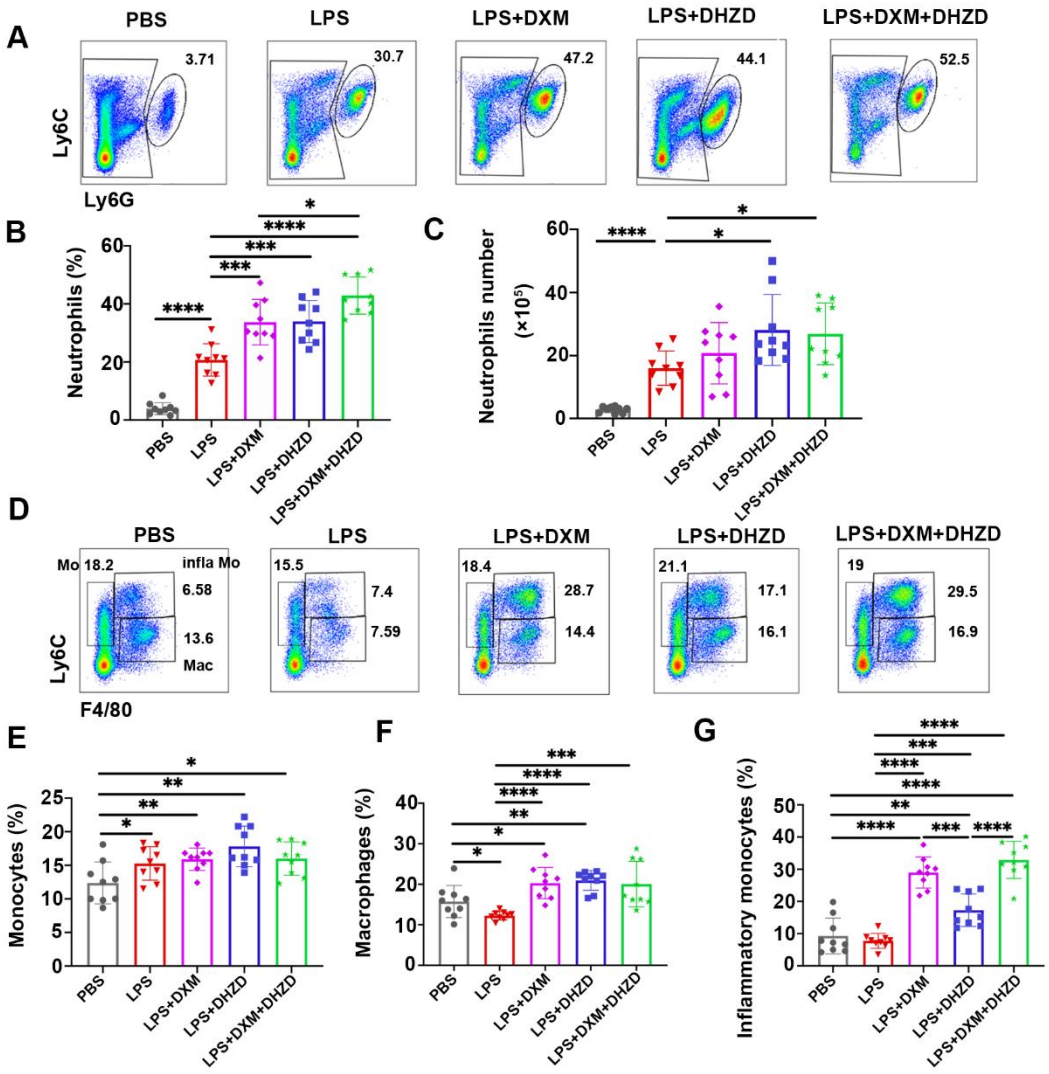

371

372 **Figure 5. DHZD increased the proportions of lung neutrophils, monocytes and macrophages**

373 **induced by LPS challenge.** Mice were injected by PBS, LPS, DXM, or DHZD, accordingly. At 12

374 h after stimulation, mice were sacrificed to collect their lung tissues and single cell suspensions

375 were prepared for FACS analysis. The proportions of lung neutrophils, monocytes and macrophages

376 in lungs were detected. One representative scatter plot per group and the proportions of neutrophils

377 (A-C). One representative scatter plot and the proportion of monocyte-macrophages (D-H). Data
378 were shown as means ± SD for each group (nine mice in each group). *, $P<0.05$, **, $P<0.01$, ***,
379 $P<0.001$, and ****, $P<0.0001$.

380 **DHZD enhanced the phagocytosis of pHrodo-labelled *E. coli* via CD36 in a**
381 **clathrin-dependent and actin-polymerized manner in macrophages**

382 PHrodo-labeled *E. coli* is a type of model bacteria that emits fluorescence only in
383 phagocytic cells because of the acidic environment. To clarify the regulatory effect of
384 DHZD on the phagocytotic ability, RAW264.7 cells were stimulated by LPS and DHZD
385 (15 μM) for 24 h. PHrodo-labeled *E. coli* was added and incubated for 1 h in dark. The
386 amount of engulfed *E. coli* in the cytoplasm was measured by Flow cytometry. DHZD
387 significantly increased the phagocytosis of pHrodo-labeled *E. coli* in RAW264.7 (Fig.
388 6A-C), suggesting that DHZD could promote the ability of bacterial phagocytosis of
389 macrophages.

390 The initiation of phagocytosis depends on the recognition and binding of host cell
391 receptors to the corresponding ligands on the surface of the pathogens. Innate immune
392 cells such as macrophages, neutrophils and dendritic cells can phagocyte pathogens
393 through caveolin-mediated endocytosis, clathrin-mediated endocytosis, pinocytosis
394 and other ways (23, 24). All the above-mentioned phagocytotic mechanisms are actin
395 dependent. Filipin III, CPZ and cytochalasin D are inhibitors of caveolin, clathrin and
396 actin, respectively. Filipin III had no effects on DHZD-promoted phagocytosis of
397 bacteria in RAW264.7 cells. CPZ could partially inhibit DHZD-promoted phagocytosis.
398 Cytochalasin D has the ability of preventing actin polymerization, and could completely

399 prevent the enhanced phagocytosis by DHZD (Fig. 6D-F).

400 Bacterial phagocytosis is usually mediated by phagocytic receptors. The
401 expression of phagocytic receptors CD36, FcγR2a, CD206, Dectin-1, CR3 and CR4
402 were detected by qRT-PCR on the surface of macrophages. From the expression screen,
403 DHZD could promote the expression of CD36 (Fig. 6G-H), at least partially accounting
404 for the increased ability of phagocytosis.

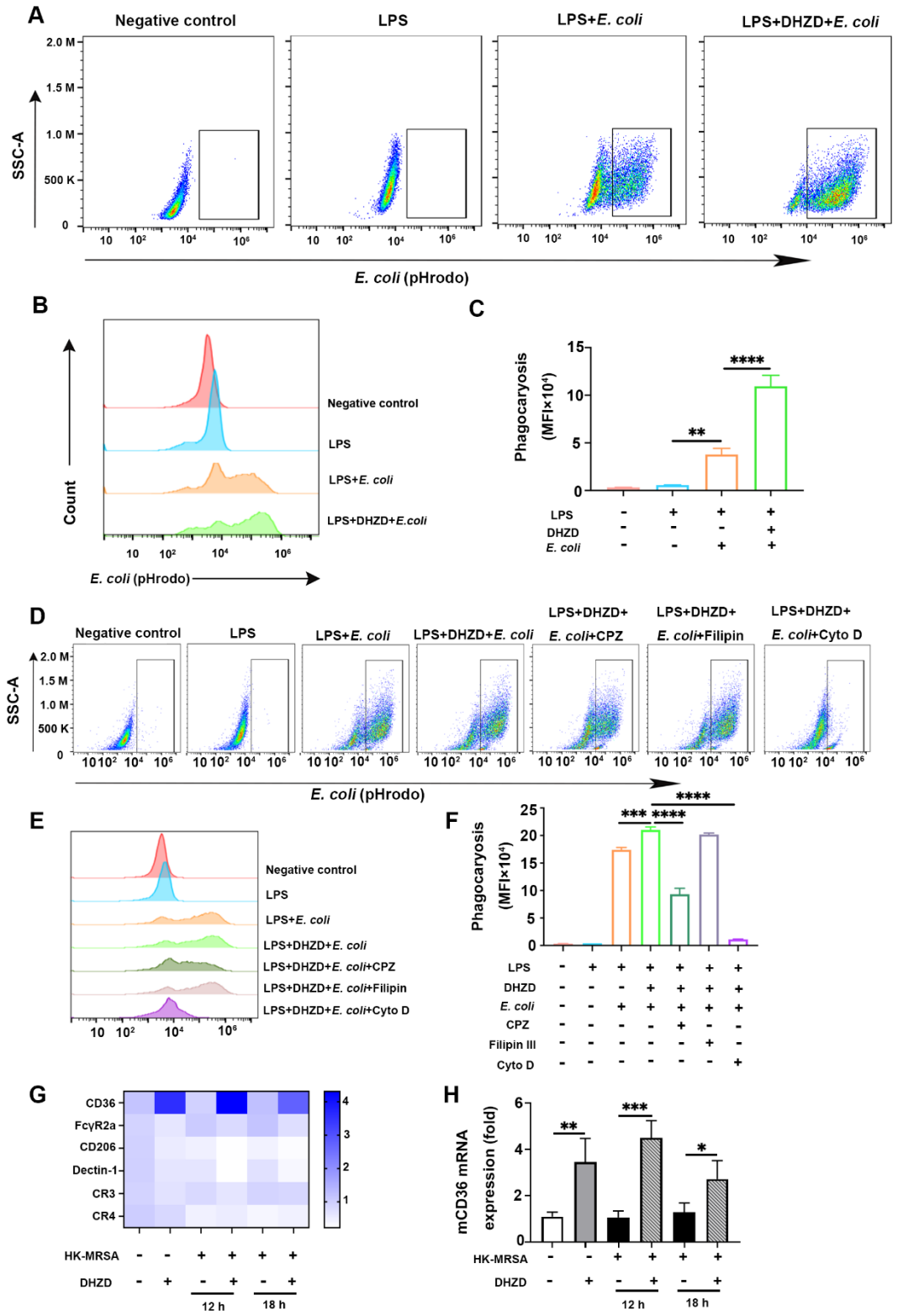

405

406 **Figure 6. DHZD enhanced the phagocytosis of pHrodo-labelled *E. coli* in a clathrin-dependent**

407 **and actin-polymerized manner and also increased the expression of CD36 in RAW264.7 cells.**

408 RAW264.7 cells were plated at 1×10^5 cells/100 μL in 96-well plates and incubated overnight. Then
409 cells were primed with LPS (100 ng/mL) along with DHZD (15 μM). After 24 h, macrophages were
410 incubated with pHrodo-labelled *E. coli* protected from light for 1 h. Cells were washed with sterile
411 PBS for three times to get rid of the bacteria outside of the cells. Then the phagocytosis of pHrodo-
412 labelled *E. coli* was quantified by FACS. One representative scatter plot out of three independent
413 experiments were shown (A). The mean fluorescence intensity (MFI) of pHrodo-labelled *E. coli*
414 swallowed by RAW264.7 cells were analyzed (B, C). RAW264.7 cells (1×10^5 cells/100 μL) were
415 seeded in 96-well plates and cultured overnight. Cells were pretreated with filipin III (3 μM), Cyto
416 D (10 μM) or CPZ (10 μM) for 30 min. Then cells were co-cultured with LPS (100 ng/mL) and
417 DHZD (15 μM) for 24 h (D-F). RAW264.7 cells were seeded (2×10^5/well) in 24-well plates and
418 incubated overnight. Cells were treated with HK-MRSA (MOI=10) separately along with DHZD
419 (15 μM) for 12 and 18 h. The expression of CD36 (G, H) were detected by PCR. Data were shown
420 as mean ± SD from three independent experiments; *, P <0.05, **, P <0.01, ***, P <0.001, and
421 ****, P <0.0001.

422 **DHZD inhibited LPS-stimulated activation of PI3K/Akt/p70S6K pathway**

423 Our results have demonstrated that DHZD effectively reduced LPS-induced
424 inflammatory response. The results showed that DHZD inhibited LPS-induced
425 phosphorylation of Akt at Ser473 and Thr308 and subsequent p70S6K at Thr389.
426 Meanwhile, DHZD had no effects on the activation of ERK and p38 MAPK signaling
427 pathways (Fig. 7A-E).

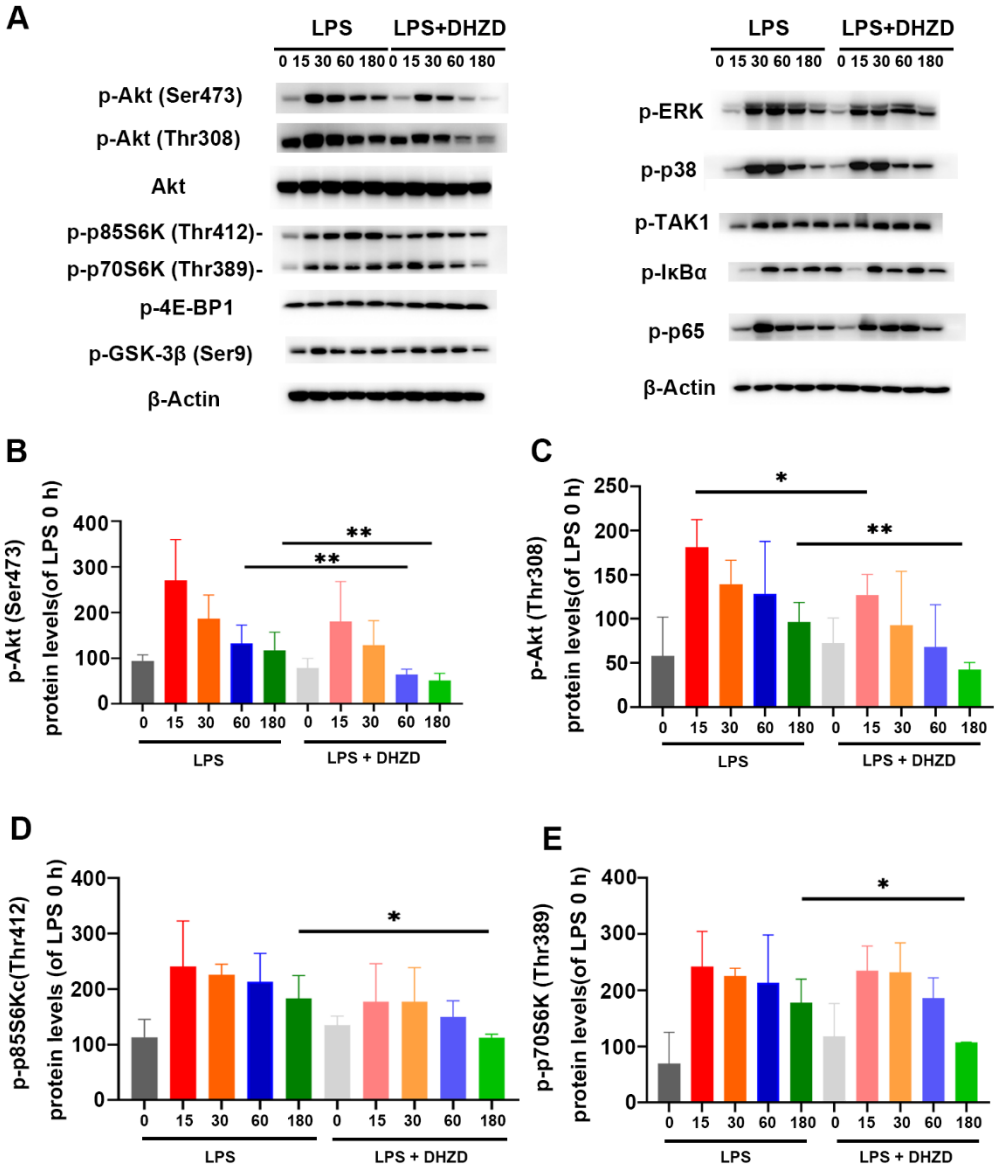

Figure 7. DHZD inhibited LPS-stimulation of PI3K/Akt activation. RAW264.7 cells (1×10^6 cells/well) were seeded in 6-well plates overnight and stimulated with LPS (100 ng/mL) with or without DHZD (15 μM) for a certain period of time. Total protein of cells was detected by Western blot (A-E). Phospho-Akt (Ser 473), phospho-Gsk-3β (Ser9), phospho-ERK, phospho-p38, phospho-IκBα (Ser32/36), phospho-p65 (Ser536) and β-Actin in RAW264.7 were verified by Western blot. Data were shown as mean ± SD from three independent experiments; *, P <0.05, **, P <0.01, ***, P <0.001, and ****, P <0.0001.

436 **DHZD reversed hypothermia, tissue damage, and over-activated inflammation**
437 **caused by CRKP**

438 LPS is the main component of the cell wall of G^- bacteria. CRKP is one of the
439 most troublesome G^- bacteria causing severe infection and sepsis in emergency
440 department or intensive care unit (ICU). Fever is usually one of the most important
441 symptoms of infection (25). There are variable thermoregulatory responses in sepsis,
442 including fever and hypothermia (26). According to the analysis of clinical data, the
443 mortality rate of septic patients with hypothermia is much higher than those with fever
444 (27).

445 In order to clarify the protective effects of DHZD on CRKP-infected mice, a septic
446 mouse model was established by the injection of CRKP intraperitoneally, which is
447 sensitive to LVX. LVX was used as a positive control antibiotic in our mouse model.
448 Infrared thermal imaging thermometer were also used to monitor body temperature of
449 mice before and after CRKP challenge. Compared with the model group, DHZD-L
450 group restored the average body temperature by 1.3 ℃, and DHZD-H group restored
451 the average body temperature by 3.1 ℃. The results suggested that DHZD had an
452 impressive protective effect on the recovery of body temperature (Fig. 8A-B).
453 Compared with the PBS group, the lung tissue of mice in the CRKP group showed
454 obvious infiltration of inflammatory cells, a large amount of fluid exudation in the
455 alveoli, and pulmonary interstitial thickening. Inflammatory cell infiltration, swelling
456 and necrosis of hepatocytes, fragmentation and lysis of some nuclei, and destruction of
457 hepatic plate structure were observed in the liver. DHZD ameliorated lung and liver

tissue damage. A pathological score of lung tissue, as measured by pulmonary edema, alveolar infiltration, and pulmonary vasculitis, showed a protective effect of DHZD administration against pathological damage to the tissue (Fig. 8C-D).

In vitro stimulation of primary peritoneal macrophages of mice with HK-CRKP showed that DHZD could reduce the secretion of IL-6, TNF-α, MCP-1, IL-1β and IL-10 in a dose-dependent manner, but had no obvious influence on MIP-2 secretion (Fig. 8E-J).

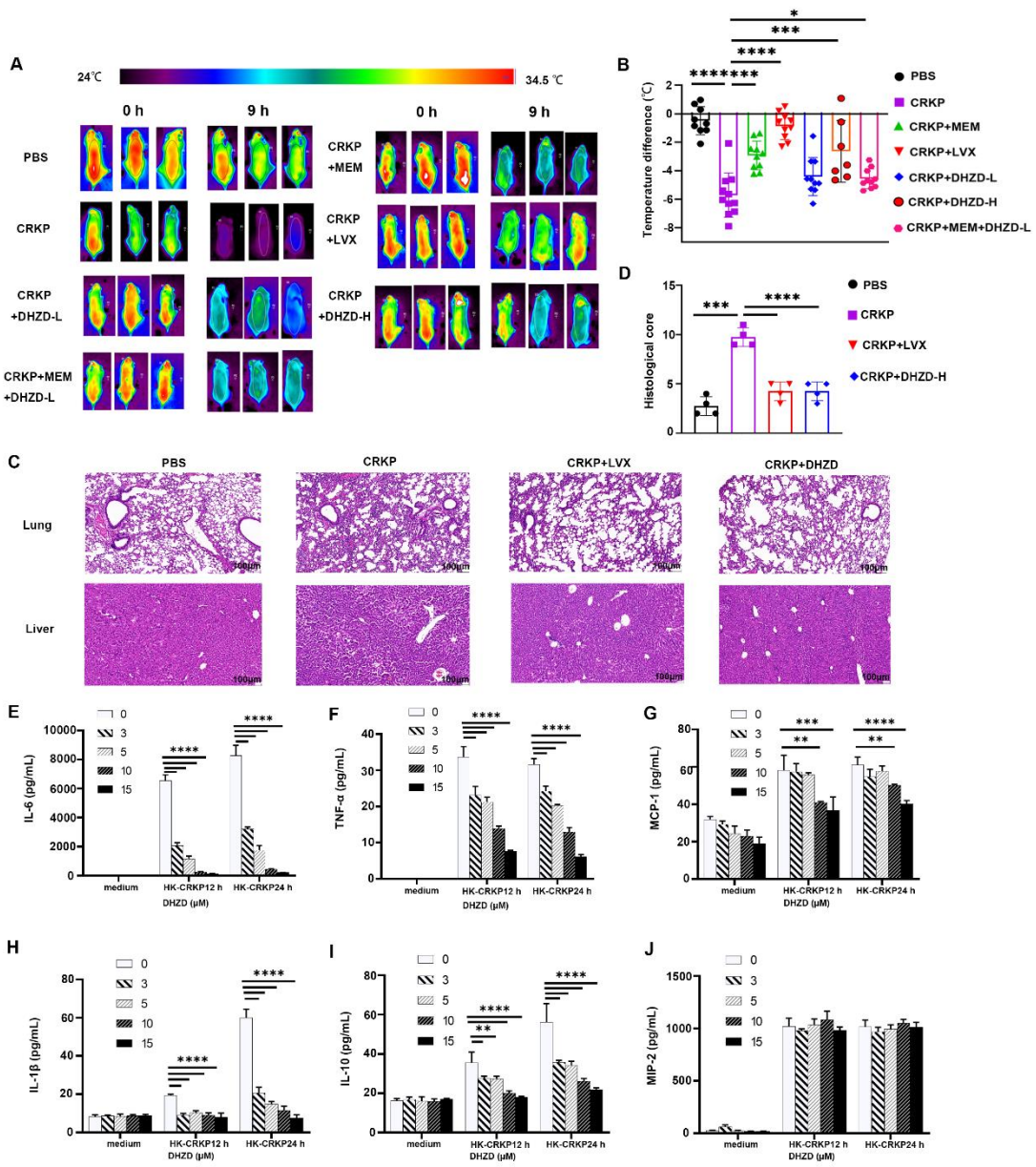

Figure 8. DHZD reversed hypothermia, tissue damage, and inflammation caused by CRKP. C57BL/6J female mice were randomly divided into 6 groups (10 mice/group). All groups of mice were challenged by lethal dose of CRKP and corresponding agents, respectively. Temperature difference (A, B). H&E staining of lung and liver (200×) (C). Scale bar 100 μm, and the histological core of lung (D). Mouse primary macrophages were plated (3.5×10^5 cells/500 μL) in 24-well plates at the day before stimulated. Cell culture supernatants were collected at 12 and 24 h after co-stimulation of different concentrations of DHZD and HK-CRKP (MOI=10), and the concentrations

473 of IL-6 (E), TNF-α (F), MCP-1 (G), IL-1β (H), IL-10 (I) and MIP-2 (J) were measured by ELISA.
474 Data were shown as mean ± SD from three independent experiments. *, $P<0.05$, **, $P<0.01$, ***,
475 $P<0.001$, and ****, $P<0.0001$.

476 **Discussion**

477 AMR is an increasingly difficult problem for human beings, and it is also the main
478 cause accounting for the high mortality rate of septic patients. After bacterial infection,
479 the invading bacteria encounter host innate immune system at the beginning, and innate
480 cells "sense" the pathogens by recognizing pathogen-associated molecular patterns
481 (PAMPs) via pattern recognition receptors (PRRs). In most cases, the innate immune
482 response can help to eliminate the invading bacteria. When the bacteria prevail in host,
483 the immune response may become unbalanced (28, 29), further triggering the
484 overwhelming production of cytokines, such as TNF-α, IL-1β, IL-6, etc. (30). Then, the
485 excessive inflammatory response promotes the activation of the coagulation system and
486 the formation of microthrombosis in blood vessels, leading to disseminated
487 intravascular coagulation (DIC) (31, 32).

488 "Cytokine storm" is the main cause of death in septic patients with multiple organ
489 failure. The levels of inflammatory cytokines IL-1β, IL-6, IL-12 and IL-17 are usually
490 high in septic patients. In a mouse model of cecal ligation and puncture, the
491 administration of anti-IL-6 antibody reduced the expression of C5a and improved the
492 survival of the mice (33). In a study of community-acquired pneumonia, the mean
493 serum concentration of IL-6 from severe septic patients was 54.1 pg/mL, compared
494 with 36.5 pg /mL from patients who do not develop severe sepsis (34). Similarly, the

495 serum levels of IL-1β in deceased septic patients were about 2-10 times higher than
496 those in surviving septic patients. These clinical data suggested that high concentrations
497 of IL-6 or IL-1β may be closely related to poor prognosis (35). TNF-α is not only
498 involved in cytokine storm but also responsible for the induction of hypothermia and
499 high mortality in sepsis (36). In a study of *E. coli*-induced sepsis in baboons, treatment
500 with anti-TNF antibody at 2 h before infection protected vital organ damage and
501 reduced mortality (37). From the clinical experience, the downregulation of the
502 excessive cytokine expression can alleviate tissue damage, reduce the conversion rate
503 from mild to severe diseases, and thus improve the survival status of sepsis. DHZD
504 could inhibit the over-activated inflammatory response (IL-6, TNF-α, IL-1β, IL-12,
505 IFN-β and IL-10, etc.) in RAW264.7 cells, mouse primary peritoneal macrophages and
506 BMDMs after the stimulation of bacteria or bacterial mimic. In the early stage of sepsis,
507 DCs could also produce a series of inflammatory factors (such as IL-6, TNF-α, IL-12
508 and chemokines) after bacterial phagocytosis (38). Elevated IL-12 is also found during
509 sepsis, which induces the differentiation of naive T cells into helper T cell (Th1) and
510 the activation of NK cells, contributing to the formation of cytokine storm (39). DHZD
511 downregulated the production of IL-6, TNF-α and IL12p70 in DCs, suggesting that it
512 may also down-regulate cytokine storm via impairing subsequent T cell over-activation.
513 In LPS-induced septic mouse model, DHZD showed an impressive anti-
514 inflammatory role and alleviated lung, liver and kidney damage, improving the survival
515 rate. Both of the examined concentrations of DHZD showed protective effects *in vivo*.
516 The survival rate of LPS + DHZD + DXM group was 100 %, which was better than

517 that of LPS + DXM group (60 %), suggesting that the combination of DHZD and DXM
518 may have a potential synergistic protective effect to treat sepsis.

519 All of TNF-α, interleukin, and interferon γ can induce hypothermia via regulating
520 thermotaxic center of the brain (40, 41). During infection, the activity of animals is
521 reduced, which can also lead to the appearance of hypothermia (42). In sepsis,
522 compared with patients in the fever group, patients in the hypothermia group had central
523 nervous system dysfunction (88 % vs 60 %), elevated serum bilirubin concentration
524 (35 % vs 15 %), prolonged prothrombin time (50 % vs 23 %), shock (94 % vs 61 %),
525 nonrecovery from shock (66 % vs 26 %), and death (62 % vs 26 %) (43). In our current
526 study, DHZD protected the loss of body temperature in CRKP-induced septic mouse
527 model (-5.7 ℃ vs -2.6 ℃) compared to those of CRKP group mice, hinting that DHZD-
528 treated infective mice have better prognosis.

529 The load of pathogens is usually related to the severity of infectious diseases.
530 Macrophage is a ubiquitous phagocytic cell type of innate immune system, and is
531 involved in defensive inflammatory response and pathogen clearance during bacterial
532 infection (44, 45). Besides macrophages, neutrophils and DCs are also important
533 phagocytic cells in the body, which can phagocytize bacteria and decrease bacterial load.
534 In our study, macrophages were used as a cell model to investigate whether DHZD has
535 an ability to influence the cellular phagocytosis. DHZD was shown to promote the
536 phagocytic ability of bacteria of macrophages in a clathrin-and actin-dependent manner.
537 CD36, a member of class B scavenger receptor family, is expressed on cells such as
538 monocytes, macrophages, endothelial cells, and adipocytes (34). The up-regulation of

539 CD36 expression by DHZD, might at least partially provide explanations for the
540 enhanced phagocytosis of macrophages. Not only the expression of phagocytic
541 receptors of phagocytes, but also the proportions and numbers of neutrophils and
542 monocytes/macrophages in lungs were increased by DHZD after LPS challenge,
543 suggesting that DHZD might contribute to a quick control of bacterial load at early
544 stage of infection through phagocytosis. Accordingly, DHZD might play a protective
545 role during bacterial infection and decrease organ damage.

546 As a member of innate immune cells, DC plays an important role on the line of
547 defense against pathogen. Immature DCs have a strong phagocytic ability. As it matures,
548 the phagocytic ability of DC is decreased and the expression of MHC II molecules and
549 co-stimulatory molecules (CD86, CD80 and CD40) are increased, accompanied by the
550 increased antigen presenting ability to evoke T cell activation (46-48). The down-
551 regulated expression of co-stimulatory molecules (CD80, CD86 and CD40) and MHC
552 II by DHZD keeps DC in an immature status, and might maintain its strong phagocytic
553 ability of bacteria and preventing the over-activation of T cells.

554 The PI3K/Akt signaling pathway also acts as an important regulator of cytokine
555 production after TLR4 ligation with LPS during G^- bacterial infection (49). Previous
556 studies have shown that the inhibition of PI3K/Akt activation in DCs or macrophages
557 reduces the secretion of pro-inflammatory factors (IL-6, TNF-α, IL-12 and IL-1β, etc.)
558 while promotes the secretion of the anti-inflammatory factor IL-10 in TLR2 and TLR4
559 signaling (50, 51). DHZD inhibited the activation of PI3K/Akt/p70S6K signaling
560 pathway, but had no influence on the activation of ERK and p38 MAPK signaling

pathways, accounting for its anti-inflammatory role.

In conclusion, DHZD has an obvious anti-inflammatory effect *in vitro* and *in vivo* via targeting the host immune response. It may be a potential therapeutic drug for the treatment of sepsis caused by bacterial infection and even drug-resistant bacterial infection. Whether the phagocytic ability of bacteria besides *E. coli* could also be increased by DHZD needs further experiments. Interestingly, the combination of DHZD and DXM is expected to improve the survival rate of septic mice, hinting that DHZD might be a potential adjuvant drug candidate for the treatment of sepsis.

Acknowledgments

This work was supported by grants from National Key Research and Development Program of China (2021YFE0200900), National Natural Science Foundation of China (82073901, 82073726), Shanghai Municipal Science and Technology Major Project (ZD2021CY001), the Key Research and Development Program of Shaanxi Province (2020SF-226), three-year Action Plan for Shanghai TCM Development and Inheritance Program [ZY (2021-2023)-0401 and ZY (2021-2023)-0103]. Traditional Chinese Medicine Research Project of Shanghai Municipal Health Commission (2022QN043). We are thankful for Dr. Yi-jian Chen from Huashan Hospital affiliated to Fudan University to provide Carbapenem-resistant *Klebsiella pneumoniae* (CRKP, HS11286). Thank Ali Mollahassani for language polishing of this paper.

Author contribution

Yue-juan Zheng designed the experiments. Xiang-yang Qin modified and provided DHZD. Ying-xiang Zou, Tian-nan Xiang, Huan Zhang, Yu-he Ma, Xiao Wu, Qi-lin

Huang, Biao Lei and Jing-wen Mu performed the laboratory assays. Ying-xiang Zou, Tian-nan Xiang, Huan Zhang and Yu-he Ma analyzed the data. Yue-juan Zheng and Ying-xiang Zou wrote the manuscript. Tian-nan Xiang and Xiang-yang Qin contributed to manuscript revision. All authors read and approved the manuscript.

Supplementary information

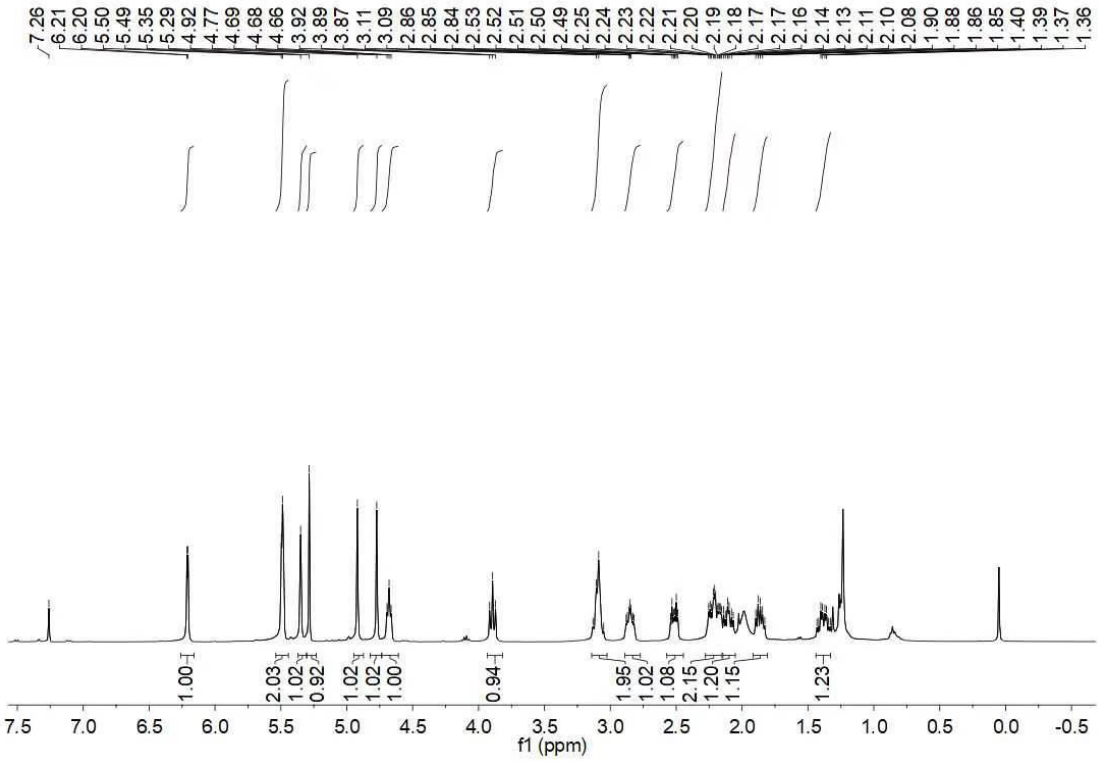

Figure S1. Plot of the spectral data of DHZD.

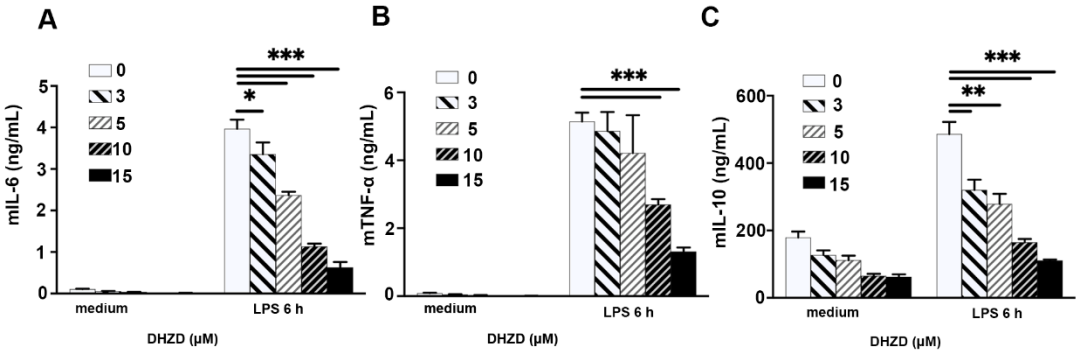

Figure S2. DHZD decreased the secretion of LPS- induced IL-6, TNF-α, MCP-1 and IL-10 in BMDMs. Tibias and femurs were obtained from C57BL/6 mice and differentiated into bone marrow

derived macrophages (BMDMs) by the addition of L929 conditional media for 5 constitutive days. Cells were seeded (3.5 × 10^5 cells/well) in 24-well plates and then stimulated by LPS (100 ng/mL) and DHZD for 6 h. The secretion of IL-6 (A), TNF-α (B) and IL-10 (C) were detected by ELISA. Data were shown as mean ± SD from three independent experiments. *, P <0.05, **, P <0.01, and ***, P <0.001.

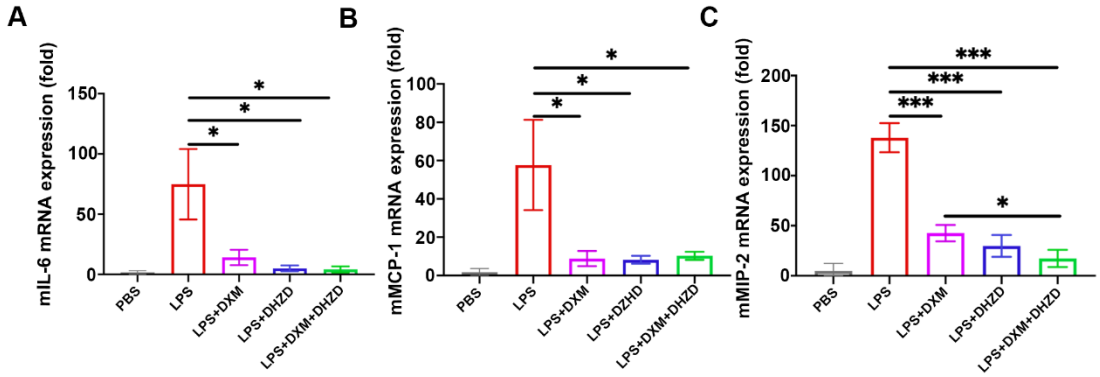

Figure S3. DHZD deceased the expression of inflammatory response in lung of LPS-induced acute peritonitis mice. C57BL/6J mice were randomly divided into 5 groups (9 mice/group). All groups of mice were stimulated with LPS (10 mg/kg) and interfered with DXM (5 mg/kg), DHZD (10 mg/kg, 40 mg/kg) and their combination according to the groups. After 12 hours of intervention, the mice were sacrificed. The mRNA expression of IL-6 (A), MCP-1(B) and MIP-2 (C) in lung tissues were detected by qRT-PCR. Data were shown as mean ± SD of three mice per group. *, P <0.05, and ***, P <0.001.

Reference:

1. Mu A, Klare WP, Baines SL, Ignatius Pang CN, Guérillot R, Harbison-Price N, Keller N, Wilksch J, Nhu NTK, Phan MD, Keller B, Nijagal B, Tull D, Dayalan S, Chua HHC, Skoneczny D, Koval J, Hachani A, Shah AD, Neha N, Jadhav S, Partridge SR, Cork AJ, Peters K, Bertolla O, Brouwer S, Hancock SJ, Álvarez-Fraga L, De Oliveira DMP, Forde B, Dale A, Mujchariyakul W, Walsh CJ, Monk I, Fitzgerald A, Lum M, Correa-Ospina C, Roy Chowdhury P, Parton RG, De Voss J, Beckett J, Monty F, McKinnon J, Song X, Stephen JR, Everest M, Bellgard MI, Tinning M, Leeming M, Hocking D, et al. 2023. Integrative omics identifies conserved and pathogen-specific responses of sepsis-causing bacteria. Nat

615 Commun 14:1530.
616 2. Singer M, Deutschman CS, Seymour CW, Shankar-Hari M, Annane D, Bauer M, Bellomo
617 R, Bernard GR, Chiche JD, Coopersmith CM, Hotchkiss RS, Levy MM, Marshall JC, Martin
618 GS, Opal SM, Rubenfeld GD, van der Poll T, Vincent JL, Angus DC. 2016. The Third
619 International Consensus Definitions for Sepsis and Septic Shock (Sepsis-3). Jama 315:801-
620 10.
621 3. Gersh, B. JJYoC. 2011. Population Trends in the Incidence and Outcomes of Acute
622 Myocardial Infarction.
623 4. Siegel R, Ma J, Zou Z, Jemal A. 2014. Cancer statistics, 2014. CA Cancer J Clin 64:9-29.
624 5. Fleischmann C, Scherag A, Adhikari NK, Hartog CS, Tsaganos T, Schlattmann P, Angus DC,
625 Reinhart K. 2016. Assessment of Global Incidence and Mortality of Hospital-treated Sepsis.
626 Current Estimates and Limitations. Am J Respir Crit Care Med 193:259-72.
627 6. Adhikari NK, Fowler RA, Bhagwanjee S, Rubenfeld GD. 2010. Critical care and the global
628 burden of critical illness in adults. Lancet 376:1339-46.
629 7. Compston J. 2018. Glucocorticoid-induced osteoporosis: an update. Endocrine 61:7-16.
630 8. Cutolo M, Seriolo B, Pizzorni C, Secchi ME, Soldano S, Paolino S, Montagna P, Sulli A. 2008.
631 Use of glucocorticoids and risk of infections. Autoimmun Rev 8:153-5.
632 9. Savva A, Roger T. 2013. Targeting toll-like receptors: promising therapeutic strategies for
633 the management of sepsis-associated pathology and infectious diseases. Front Immunol
634 4:387.
635 10. O'Neill LA, Bowie AG. 2007. The family of five: TIR-domain-containing adaptors in Toll-
636 like receptor signalling. Nat Rev Immunol 7:353-64.
637 11. Schumann J. 2016. It is all about fluidity: Fatty acids and macrophage phagocytosis. Eur J
638 Pharmacol 785:18-23.
639 12. Groves E, Dart AE, Covarelli V, Caron E. 2008. Molecular mechanisms of phagocytic uptake
640 in mammalian cells. Cell Mol Life Sci 65:1957-76.
641 13. Fridman WH. 1991. Fc receptors and immunoglobulin binding factors. Faseb j 5:2684-90.
642 14. Ninković J, Roy S. 2012. Morphine decreases bacterial phagocytosis by inhibiting actin
643 polymerization through cAMP-, Rac-1-, and p38 MAPK-dependent mechanisms. Am J
644 Pathol 180:1068-1079.
645 15. An H, Hou J, Zhou J, Zhao W, Xu H, Zheng Y, Yu Y, Liu S, Cao X. 2008. Phosphatase SHP-
646 1 promotes TLR- and RIG-I-activated production of type I interferon by inhibiting the
647 kinase IRAK1. Nat Immunol 9:542-50.
648 16. Zheng Y, An H, Yao M, Hou J, Yu Y, Feng G, Cao X. 2010. Scaffolding adaptor protein
649 Gab1 is required for TLR3/4- and RIG-I-mediated production of proinflammatory
650 cytokines and type I IFN in macrophages. J Immunol 184:6447-56.
651 17. Han C, Jin J, Xu S, Liu H, Li N, Cao X. 2010. Integrin CD11b negatively regulates TLR-
652 triggered inflammatory responses by activating Syk and promoting degradation of
653 MyD88 and TRIF via Cbl-b. Nat Immunol 11:734-42.
654 18. Franco-Molina MA, Mendoza-Gamboa E, Castillo-León L, Tamez-Guerra RS, Rodríguez-
655 Padilla C. 2004. Bovine dialyzable leukocyte extract protects against LPS-induced, murine
656 endotoxic shock. Int Immunopharmacol 4:1577-86.
657 19. Zheng Y, Guo Z, He W, Yang Y, Li Y, Zheng A, Li P, Zhang Y, Ma J, Wen M, Yang M, An H,
658 Ji G, Yu Y. 2012. Ephedrine hydrochloride protects mice from LPS challenge by promoting

659 IL-10 secretion and inhibiting proinflammatory cytokines. Int Immunopharmacol 13:46-
660 53.
661 20. Jiang X, Chen Y, Liu D, Shi T, Cheng X, He W, Li Y, Ryffel B, Zheng SG, Zheng Y. 2020.
662 Secoeudesma sesquiterpenes lactone A alleviates inflammation and offers adjuvant
663 protection in severe infection of carbapenem-resistant Klebsiella pneumoniae. J
664 Ethnopharmacol 252:112605.
665 21. Zhang AJ, Lee AC, Chan JF, Liu F, Li C, Chen Y, Chu H, Lau SY, Wang P, Chan CC, Poon VK,
666 Yuan S, To KK, Chen H, Yuen KY. 2021. Coinfection by Severe Acute Respiratory Syndrome
667 Coronavirus 2 and Influenza A(H1N1)pdm09 Virus Enhances the Severity of Pneumonia
668 in Golden Syrian Hamsters. Clin Infect Dis 72:e978-e992.
669 22. Ando M, Isogai K, Azami H, Hirata N, Yamazaki H, Yanagi Y. 1992. Studies on the synthesis
670 of sesquiterpene lactones, 14. Syntheses of (-)-arbusclin D and (+)-4-EPI-arbusclin D: the
671 stereochemical assignment of arbusclin D. J Nat Prod 55:1620-5.
672 23. Doherty GJ, McMahon HT. 2009. Mechanisms of endocytosis. Annu Rev Biochem 78:857-
673 902.
674 24. Ramanan V, Agrawal NJ, Liu J, Engles S, Toy R, Radhakrishnan R. 2011. Systems biology
675 and physical biology of clathrin-mediated endocytosis. Integr Biol (Camb) 3:803-15.
676 25. Walter EJ, Hanna-Jumma S, Carraretto M, Forni L. 2016. The pathophysiological basis and
677 consequences of fever. Crit Care 20:200.
678 26. Thomas-Rüddel DO, Hoffmann P, Schwarzkopf D, Scheer C, Bach F, Komann M, Gerlach
679 H, Weiss M, Lindner M, Rüddel H, Simon P, Kuhn SO, Wetzker R, Bauer M, Reinhart K,
680 Bloos F. 2021. Fever and hypothermia represent two populations of sepsis patients and
681 are associated with outside temperature. Crit Care 25:368.
682 27. Rumbus Z, Matics R, Hegyi P, Zsiboras C, Szabo I, Illes A, Petervari E, Balasko M, Marta K,
683 Miko A, Parniczky A, Tenk J, Rostas I, Solymar M, Garami A. 2017. Fever Is Associated with
684 Reduced, Hypothermia with Increased Mortality in Septic Patients: A Meta-Analysis of
685 Clinical Trials. PLoS One 12:e0170152.
686 28. van der Poll T, van de Veerdonk FL, Scicluna BP, Netea MG. 2017. The immunopathology
687 of sepsis and potential therapeutic targets. Nat Rev Immunol 17:407-420.
688 29. Takeuchi O, Akira S. 2010. Pattern recognition receptors and inflammation. Cell 140:805-
689 20.
690 30. Kang R, Chen R, Zhang Q, Hou W, Wu S, Cao L, Huang J, Yu Y, Fan XG, Yan Z, Sun X,
691 Wang H, Wang Q, Tsung A, Billiar TR, Zeh HJ, 3rd, Lotze MT, Tang D. 2014. HMGB1 in
692 health and disease. Mol Aspects Med 40:1-116.
693 31. Opal SM. 2011. Immunologic alterations and the pathogenesis of organ failure in the ICU.
694 Semin Respir Crit Care Med 32:569-80.
695 32. Tang D, Wang H, Billiar TR, Kroemer G, Kang R. 2021. Emerging mechanisms of
696 immunocoagulation in sepsis and septic shock. Trends Immunol 42:508-522.
697 33. van der Poll T, Levi M, Hack CE, ten Cate H, van Deventer SJ, Eerenberg AJ, de Groot ER,
698 Jansen J, Gallati H, Büller HR, et al. 1994. Elimination of interleukin 6 attenuates
699 coagulation activation in experimental endotoxemia in chimpanzees. J Exp Med
700 179:1253-9.
701 34. Wu HP, Chen CK, Chung K, Tseng JC, Hua CC, Liu YC, Chuang DY, Yang CH. 2009. Serial
702 cytokine levels in patients with severe sepsis. Inflamm Res 58:385-93.

703 35. Mera S, Tatulescu D, Cismaru C, Bondor C, Slavcovici A, Zanc V, Carstina D, Oltean M.
704 2011. Multiplex cytokine profiling in patients with sepsis. Apmis 119:155-63.
705 36. Leon LR, White AA, Kluger MJ. 1998. Role of IL-6 and TNF in thermoregulation and survival
706 during sepsis in mice. Am J Physiol 275:R269-77.
707 37. Tracey KJ, Fong Y, Hesse DG, Manogue KR, Lee AT, Kuo GC, Lowry SF, Cerami A. 1987.
708 Anti-cachectin/TNF monoclonal antibodies prevent septic shock during lethal
709 bacteraemia. Nature 330:662-4.
710 38. Bouras M, Asehnoune K, Roquilly A. 2018. Contribution of Dendritic Cell Responses to
711 Sepsis-Induced Immunosuppression and to Susceptibility to Secondary Pneumonia. Front
712 Immunol 9:2590.
713 39. Kilbourn RG, Griffith OW, Gross SS. 1993. Pathogenetic mechanisms of septic shock. N
714 Engl J Med 329:1427-8.
715 40. Leon LR. 2004. Hypothermia in systemic inflammation: role of cytokines. Front Biosci
716 9:1877-88.
717 41. Lang GP, Ndongson-Dongmo B, Lajqi T, Brodhun M, Han Y, Wetzker R, Frasch MG, Bauer
718 R. 2020. Impact of ambient temperature on inflammation-induced encephalopathy in
719 endotoxemic mice-role of phosphoinositide 3-kinase gamma. J Neuroinflammation
720 17:292.
721 42. Jhaveri KA, Trammell RA, Toth LA. 2007. Effect of environmental temperature on sleep,
722 locomotor activity, core body temperature and immune responses of C57BL/6J mice.
723 Brain Behav Immun 21:975-87.
724 43. Clemmer TP, Fisher CJ, Jr., Bone RC, Slotman GJ, Metz CA, Thomas FO. 1992. Hypothermia
725 in the sepsis syndrome and clinical outcome. The Methylprednisolone Severe Sepsis Study
726 Group. Crit Care Med 20:1395-401.
727 44. Gentek R, Molawi K, Sieweke MH. 2014. Tissue macrophage identity and self-renewal.
728 Immunol Rev 262:56-73.
729 45. Yan J, Horng T. 2020. Lipid Metabolism in Regulation of Macrophage Functions. Trends
730 Cell Biol 30:979-989.
731 46. Darkwah S, Nago N, Appiah MG, Myint PK, Kawamoto E, Shimaoka M, Park EJ. 2019.
732 Differential Roles of Dendritic Cells in Expanding CD4 T Cells in Sepsis. Biomedicines 7.
733 47. Rescigno M, Granucci F, Ricciardi-Castagnoli P. 1999. Dendritic cells at the end of the
734 millennium. Immunol Cell Biol 77:404-10.
735 48. Lipscomb MF, Masten BJ. 2002. Dendritic cells: immune regulators in health and disease.
736 Physiol Rev 82:97-130.
737 49. Liu Y, Pan YF, Xue YQ, Fang LK, Guo XH, Guo X, Liu M, Mo BY, Yang MR, Liu F, Wu YT,
738 Olsen N, Zheng SG. 2018. uPAR promotes tumor-like biologic behaviors of fibroblast-like
739 synoviocytes through PI3K/Akt signaling pathway in patients with rheumatoid arthritis.
740 Cell Mol Immunol 15:171-181.
741 50. Stark AK, Sriskantharajah S, Hessel EM, Okkenhaug K. 2015. PI3K inhibitors in inflammation,
742 autoimmunity and cancer. Curr Opin Pharmacol 23:82-91.
743 51. Re F, Strominger JL. 2001. Toll-like receptor 2 (TLR2) and TLR4 differentially activate
744 human dendritic cells. J Biol Chem 276:37692-9.

745